DEUTSCHES ELEKTRONEN-SYNCHROTRON DESY

DESY 81-009
February 1981

EXPERIMENTAL STUDY OF JETS IN ELECTRON-POSITRON-ANNIHILATION

by

JADE Collaboration

NOTKESTRASSE 85 · 2 HAMBURG 52

To be sure that your preprints are promptly included in the
HIGH ENERGY PHYSICS INDEX ,
send them to the following address (if possible by air mail) :

DESY
Bibliothek
Notkestrasse 85
2 Hamburg 52
Germany

DESY 81-009
February 1981

Experimental Study of Jets in Electron-Positron-Annihilation

JADE-Collaboration

W. Bartel, D. Cords, P. Dittmann, R. Eichler, R. Felst, D. Haidt, H. Krehbiel, B. Naroska, L.H. O'Neill, P. Steffen, H. Wenninger[1], Y. Zhang[2]

Deutsches Elektronen-Synchrotron DESY, Hamburg, Germany

E. Elsen, M. Helm[3], A. Petersen, P. Warming, G. Weber

II. Institut für Experimentalphysik der Universität Hamburg, Germany

S. Bethke, H. Drumm, J. Heintze, G. Heinzelmann, K.H. Hellenbrand, R.D. Heuer, J. von Krogh, P. Lennert, S. Kawabata, H. Matsumura, T. Nozaki, J. Olsson, H. Rieseberg, A. Wagner

Physikalisches Institut der Universität Heidelberg, Germany

A. Bell, F. Foster, G. Hughes, H. Wriedt

University of Lancaster, England

J. Allison, A.H. Ball, G. Bamford, R. Barlow, C. Bowdery, I.P. Duerdoth, J.F. Hassard, B.T. King, F.K. Loebinger, A.A. Macbeth, H. McCann, H.E. Mills, P.G. Murphy, H.B. Prosper, K. Stephens

University of Manchester, England

D. Clarke, M.C. Goddard, R. Marshall, G.F. Pearce

Rutherford Laboratory, Chilton, England

M. Imori, T. Kobayashi, S. Komamiya, M. Koshiba, M. Minowa, M. Nozaki, S. Orito, A. Sato, T. Suda[4], H. Takeda, Y. Totsuka, Y. Watanabe, S. Yamada, C. Yanagisawa

Lab. of Int. Coll. on Elementary Particle Physics and Department of Physics, University of Tokyo, Japan

1) On leave from CERN, Geneva, Switzerland
2) Visitor from Institute of High Energy Physics, Chinese Academy of Science, Peking, People's Republic of China
3) Present address: Texaco AG, Hamburg, Germany
4) Present address: Cosmic Ray Lab., University of Tokyo, Japan

Abstract

Data on hadron production by e^+e^--annihilation at c.m. energies between 30 GeV and 36 GeV are presented and compared with two models both based on first order QCD but using different schemes for the fragmentation of quarks and gluons into hadrons. In one model the fragmentation proceeds along the parton momenta, in the other along the colour-anticolour axes. The data are reproduced better by fragmentation along the colour axes.

In hadron production by high energy electron-positron annihilation, the momenta of the final state particles tend to be contained in a narrow double cone. This 2-jet structure is expected from the process $e^+e^- \to q\bar{q}$ with subsequent fragmentation of the virtual quarks into hadrons. Recent experiments[1,2] at c.m. energies around 30 GeV using the electron-positron storage ring PETRA have shown a fraction of the events to exhibit 3-jet structure. The angular and energy distributions as well as the production rate of 3-jet events suggest that they are due to gluon bremsstrahlung $e^+e^- \to q\bar{q}g$, as predicted by perturbative QCD[3].

The conversion of quarks and gluons into hadrons, however, is not theoretically understood and is only described by phenomenological models. In particular, it is not clear whether the directions of fragmentation, i.e. the axes with respect to which the transverse momentum is limited, coincide with the directions of the original partons[4,5] or with the directions of the colour-anticolour axes[6,7]. The present investigation aims at clarifying this question experimentally.

The analysis is based on 2892 multihadron events measured with the JADE-detector at center of mass energies between 30 GeV and 36 GeV of the e^+e^--storage ring PETRA. The detector, the trigger conditions and the criteria for the selection of hadronic events have been described in ref. 8.

The data are compared with two models[4,6]. In both models the $e^+e^- \to q\bar{q}g$ cross section is calculated to first order[3] in the quark gluon coupling constant α_s. Since the lowest order $q\bar{q}g$ cross section diverges when the $q\bar{q}$ configuration is approached, the total first order QCD cross section is divided up into $q\bar{q}$ and $q\bar{q}g$ contributions $\sigma_0(1 + \alpha_s/-) = \sigma_{q\bar{q}} + \sigma_{q\bar{q}g}$ in regions of phase space where the 3-jet events are practically indistinguishable from 2-jet events.

In the model of Hoyer et al.[4] quark, antiquark and gluon fragment independently of each other, producing final state mesons with limited momentum

transverse to the directions of the original partons. The angular and energy distribution of the mesons within a jet is parametrized according to the standard prescription of Field and Feynman[9]. Gluons are treated as quark-antiquark pairs but the gluon momentum is carried entirely by one quark which subsequently fragments.

In the Lund model[6] the fragmentation proceeds along the colour flux lines as the primary partons move apart. For $q\bar{q}g$-events, these flux lines are not strung between quark and antiquark directly, but via the gluon as intermediary (see Fig. 1a). The model is formulated in terms of strings and is kinematically equivalent to a treatment of the gluon as a collinear quark-antiquark pair (q', $\bar{q}'$) with the momentum shared equally between q' and $\bar{q}'$. Each of the two gluon components form a $q\bar{q}'$ or $q'\bar{q}$ two-jet system with the primary $\bar{q}$ or q. In the $q\bar{q}'$ and $q'\bar{q}$ rest system the mesons within these jets are distributed according to the standard prescription[9], a special treatment being made only for the leading meson at the gluon corner. Neglecting transverse momenta with respect to the $q\bar{q}'$ and $q'\bar{q}$ jet axes final state particles of the same mass are distributed along hyperbolas in the over all c.m. momentum space as sketched in Fig. 1b. The model predicts that particle distributions in the angular regions between the gluon and the quark or antiquark should be different from those for the region between the quark and the antiquark.

Monte Carlo techniques were used for both models to calculate the four momenta of the final state particles. The model parameters* used have been obtained from a fit[10] of the model of Hoyer et al. to the 30 GeV data (about 50% of the present data sample). In a second step the four momenta, which include bremsstrahlung photons from the initial leptons, were converted into the actually measured quantities, such as drifttimes, pulseheights etc., taking the imperfections of the apparatus into account. These simulated data were finally processed by the same chain of computer programs as the data actually recorded and were subjected to the same cuts.

To compare the data with the model predictions the following weighted averages of $|\cos\chi_i|$ were computed for each event:

$$\Sigma_{\parallel}^{(n)} = \sum_i |\vec{p}_i|^n \cdot |\cos\chi_i| \Big/ \sum_i |\vec{p}_i|^n, \quad (n = 0,1,2)$$

where χ_i is the angle between the particle momentum vector $\vec{p}_i$ and the sphericity axis. The summation was extended over all charged and neutral particles of an event with momenta above 100 MeV and 150 MeV, respectively. The momenta of neutral particles were determined from the energy deposited in the lead glass counters. If a charged particle was also pointing into an energy cluster the average energy deposited in the lead glass by a hadron was subtracted from the cluster energy.

The experimental distributions of $\Sigma_{\parallel}^{(n)}$ are shown in Fig. 2a. The $\Sigma_{\parallel}^{(2)}$ distribution peaks at higher values than that of $\Sigma_{\parallel}^{(1)}$, which is essentially the thrust variable, the only difference being that χ is the angle between the momentum vector and the sphericity axis rather than the thrust axis. The distribution of $\Sigma_{\parallel}^{(0)}$ is even broader. This general trend is reproduced by the two model calculations although the Lund model describes the $\Sigma_{\parallel}^{(1)}$- and especially the $\Sigma_{\parallel}^{(0)}$-distribution significantly better. In Fig. 2b and Fig. 2c the $q\bar{q}$- and the $q\bar{q}g$-part**) of the theoretical distributions are shown separately. The two models predict different $q\bar{q}g$-distributions, though their $q\bar{q}$-distributions are quite similar.

These differences are qualitatively expected. In a $q\bar{q}g$-configuration as sketched in Fig. 1b, the average number and the average momenta of particles produced in the angular range between the antiquark and the gluon is larger for fragmentation along the colour axes than for fragmentation along the parton directions. The inclusion of these particles therefore yields a more two-jet like configuration in the Lund model.

Another specific prediction of this model is the production of more particles in the angular region between the quark and the gluon (Fig. 1b) than between

the two quarks. To look for this asymmetry in the experimental data, events showing a 3-jet structure are selected: For a global classification the eigenvalues Q_1, Q_2, Q_3 ($Q_1 \leq Q_2 \leq Q_3$; $Q_1 + Q_2 + Q_3 = 1$) of the normalized sphericity tensor are used. For details we refer to ref. 2. By demanding a planarity $Q_2 - Q_1 \geq 0.07$ and an aplanarity $Q_1 \leq 0.06$ we separate 484 planar events from 2-jet like events and possibly 4-jet like events. The triplicity method[11] is used to identify 3 jets of particles within a planar event and to determine the jet direction vectors. Events in which one or more of the jets contain fewer than 4 particles or an energy of less than 2 GeV are rejected. 326 events meet these criteria. The three jets are ordered according to the angles between their direction vectors, projected into the event plane, as sketched in Fig. 1c). The event plane is defined by the two eigenvectors of the sphericity tensor corresponding to the eigenvalues Q_3 and Q_2.

Fig. 3a shows angular distributions of the particles from these 3-jet events. The average number of charged and neutral particles per event is plotted as a function of the normalized projected angle θ_i/θ_{ik}, where θ_i and θ_{ik} are defined in Fig. 1c. The two model predictions are also shown in Fig. 3a. The gluon momentum vector, according to the Lund model, is closest to the jet direction vector #1, #2 and #3 in about 12%, 22% and 51% of the events, respectively. The remaining 15% of the events are 3-jet structures faked by $q\bar{q}$-events. (In the Hoyer model the corresponding numbers are 9%, 22%, 49% and 20%.)

Apart from the region between jets #1 and #2 both models describe the data reasonably well. In this region, which is the region between the two quark jets for the majority of events, the model of Hoyer et al. predicts more particles than the Lund model. As shown in Fig. 3b, this difference between the two models is enhanced if the simulated jets are ordered such as to make jet #3 always the gluon jet. In this angular range the experimental data (Fig. 3a) are in reasonable agreement with the Lund model but not with the model of Hoyer et al..

Since this difference is caused by the Lorentz transformation of the two-jet subsystem from its own c.m.s. to the overall c.m.s., it ought to be more pronounced for particles with larger $m^2+p_{out}^2$, where p_{out} is the momentum component normal to the event plane. As a measure of the asymmetry the ratio of the number of

particles in the central range $0.3 \leq \theta_i/\theta_{ik} \leq 0.7$ between jet #1 and #3 to the number between jet #1 and #2 is taken. This ratio is listed in Table 1 for all particles and separately for those with $p_{out} < 0.2$ GeV and $p_{out} > 0.2$ GeV, together with the corresponding model predictions. The ratio for particles identified as K-mesons are also given in Table 1 . Charged K-mesons with momenta $p < 0.7$ GeV are identified by the measurement of their energy loss[12]. In spite of the rather large statistical errors, the data do exhibit an increase of the asymmetry with increasing $m^2+p_{out}^2$ and again, a better agreement with the Lund model than with the model of Hoyer et al.. The same is true for the ratio of $\sum_i |\vec{p}_i^{in}|$, shown in the last row of table 1, where the summation is carried out over all particles within the above angular ranges and $\vec{p}^{in}$ is the momentum component in the event plane.

In summary: Interpreting our data by first order QCD we conclude, that fragmentation along the colour-anticolour axes resembles the structures of the actual parton-hadron conversion more closely than fragmentation along the parton momenta. This observation should be taken into account when correlating jet directions with parton directions. It also implies that gluons 'fragment' differently from quarks.

We are indebted to the PETRA machine group for their excellent support during the experiment and to all the engineers and technicians of the collaborating institutions who have participated in the construction and maintenance of the apparatus. We would like to thank A. Ali, H. Joos, G. Kramer, E. Pietarinen, G. Schierholz and T. Sjöstrand for useful discussions. This experiment was supported by the Bundesministerium für Forschung und Technologie, by the Education Ministry of Japan and by the UK Science Research Council through the Rutherford Laboratory. The visiting groups at DESY wish to thank the DESY directorate for their hospitality.

Footnotes

*) The following parameters were used for both models:
The primordial fragmentation function is $f(z) = 1 - a + 3a(1-z)^2$ with $a = 0.5$ for the u, d and s quarks, $a = 0$ for the heavy quarks, and (Hoyer model only) $a = 1$ for the quark originating from the gluon. A production ratio of secondary u, d and s quarks of 2:2:1 and a fraction of pseudoscalar mesons among the produced mesons of 50% are used. The momenta of the secondary quarks transverse to the fragmentation axis were distributed according to $d\sigma/d^2\underline{p}_\perp \sim \exp(-p^2/2\sigma_q^2)$ with $\sigma_q = 0.33$ GeV. The value of the strong coupling constant used is given by

$$\alpha_s = \frac{12\pi}{(33-2n_f)\ln(s/\Lambda^2)}$$

with $\Lambda = 0.3$ GeV and $n_f = 5$.

**) The border line between $q\bar{q}$ and $q\bar{q}g$-events is different in the two models; $q\bar{q}g$-events being 26% of the total in the Hoyer model and 52% in the Lund model. For the purpose of comparison in Fig. 2c however only events from regions of the $q\bar{q}g$-phase space populated by both models were accepted. The events omitted from the Lund sample are 2-jet like.

	Particles	Data	Models	
			Hoyer et al.	Lund
Ratio of number of particles	all	1.35 ± 0.09	1.08 ± 0.04	1.34 ± 0.06
	p^{out} < 0.2 GeV	1.23 ± 0.1	1.02 ± 0.05	1.29 ± 0.07
	p^{out} > 0.2 GeV	1.6 ± 0.2	1.20 ± 0.09	1.43 ± 0.12
	K	2.2 ± 0.7	0.89 ± 0.2	1.74 ± 0.4
Ratio of momenta	all	1.51 ± 0.1	1.18 ± 0.04	1.52 ± 0.07

Table 1

The ratio of the number of particles within $0.3 \leq \theta_i/\theta_{ik} \leq 0.7$ between jet # 3 and # 1 to the corresponding number between jet # 1 and # 2, together with the statistical uncertainties. In the last row the ratio of $\sum_i |\vec{p}_i^{in}|$ is given, where the summation is extended over all particles within the above angular ranges and $\vec{p}^{in}$ is the momentum component in the event plane.

Figure Captions

Fig. 1 Sketch of the quark and gluon velocities and of the colour-anticolour axes (a). Fragmentation along these axes, neglecting transverse momenta, yields particles of the same mass distributed in momentum space along two hyperbolas, as indicated in (b). The broadening due to different masses and transverse momenta is also indicated. The ordering scheme of the observed jets is sketched in (c). θ_{ik} is the angle between the jet axes # i and # k projected onto the event plane.

Fig. 2 The distributions of $\Sigma_{/\!/}^{(0)}$, $\Sigma_{/\!/}^{(1)}$ and $\Sigma_{/\!/}^{(2)}$ defined in the text as obtained from the data and predicted by the models (a). The model predictions for the $q\bar{q}$-part and the $q\bar{q}g$-part are shown separately in (b) and (c), respectively.

Fig. 3 The average number of particles per event between the indicated jet axes versus the normalized projected angle. The data together with the corresponding model predictions are shown in (a), the model predictions, ordered for quark and gluon jets, in (b).

References

1) TASSO-Collaboration, R. Brandelik et al., Phys. Lett. 86B (1979) 243
MARK J - Collaboration, D.P. Barber et al., Phys. Rev. Lett. 43 (1979) 830
PLUTO-Collaboration, Ch. Berger et al., Phys. Lett. 86B (1979) 418

2) JADE-Collaboration, W. Bartel et al., Phys. Lett. 91B (1980) 142

3) J. Ellis, M.K. Gaillard and G.G. Ross, Nucl. Phys. B111 (1976) 253
G. Kramer, G. Schierholz and J. Willrodt, Phys. Lett. 78B (1978) 249

4) P. Hoyer, P. Osland, H.E. Sander, T.F. Walsh and P.M. Zerwas,
Nucl. Phys. B616 (1979) 349, heavy quarks have been incorporated
by T. Meyer (private communication) using the decay matrix elements
given by
A. Ali, J.G. Körner, G. Kramer, J. Willrodt, Z. Phys. C1 (1979) 203

5) A. Ali, E. Pietarinen, G. Kramer, J. Willrodt, Phys. Lett. 93B (1980) 155

6) B. Andersson, G. Gustafson, T. Sjöstrand, Phys. Lett. 94B (1980) 211
and earlier references quoted therein,
for details see T. Sjöstrand LU TP 80-3, April 1980 and Errata to LUTP 80-3

7) J. Randa, Phys. Rev. Lett. 43 (1979) 602
I. Montvay, Phys. Lett. 84B (1979) 331

8) JADE-Collaboration W. Bartel et al., Phys. Lett. 88B (1979) 171

9) R.D. Field and R.P. Feynman, Nucl. Phys. B136 (1978) 1

10) JADE-Collaboration, presented by S. Yamada to be published in
"Proceedings of the XXth International Conference on High Energy Physics,
Madison, Wisconsin 1980"

11) S. Brandt and H. Dahmen, Z. Phys. C1 (1979) 61 and references therein.
For the triplicity calculation we use the ordering scheme described
in S.L. Wu and G. Zobernig, Z. Phys. C2 (1979) 107

12) JADE-Collaboration W. Bartel et al., Z. Phys. C6 (1980) 296

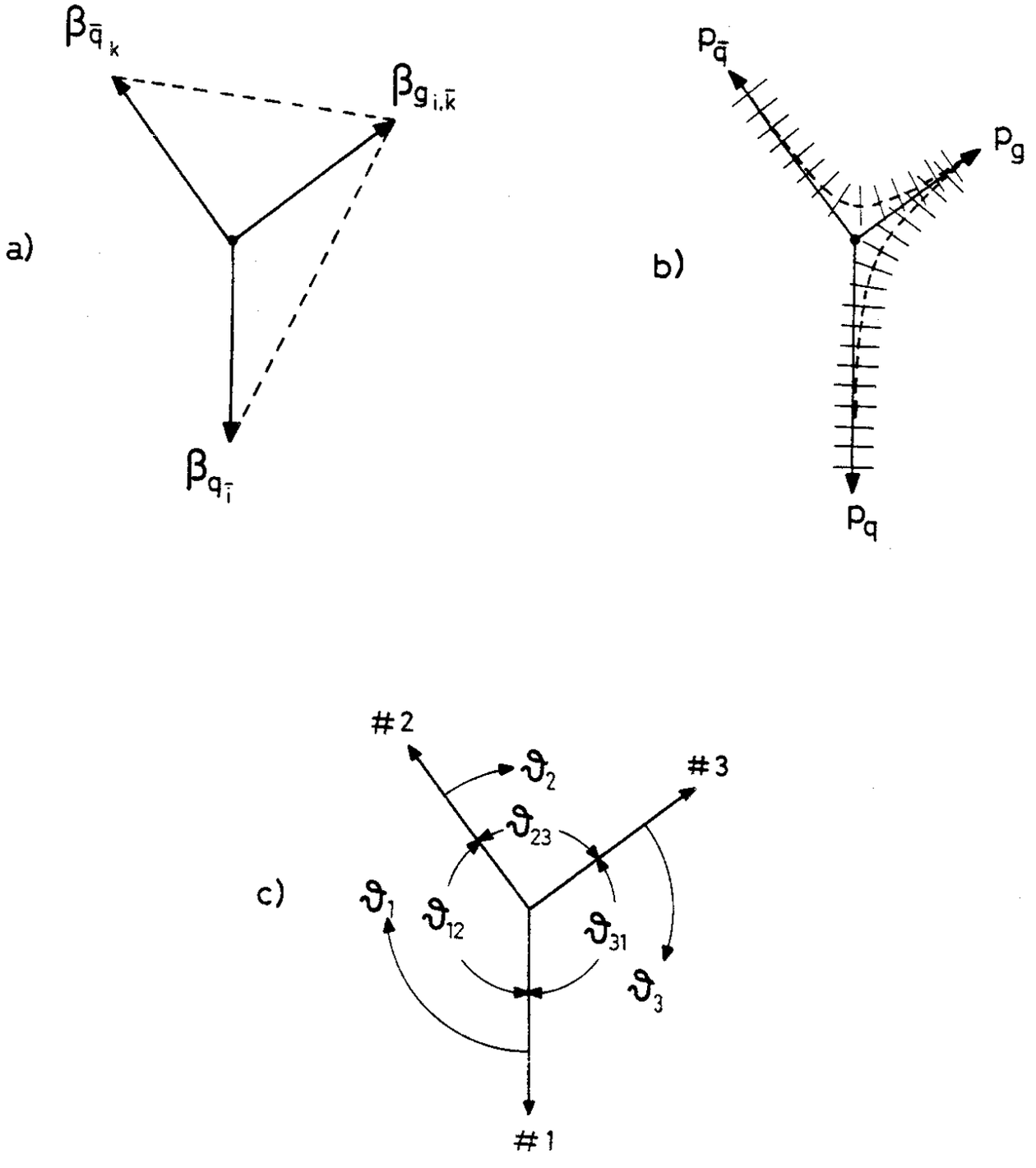

$$\vartheta_{12} \gg \vartheta_{31} \gg \vartheta_{23}$$

Fig. 1

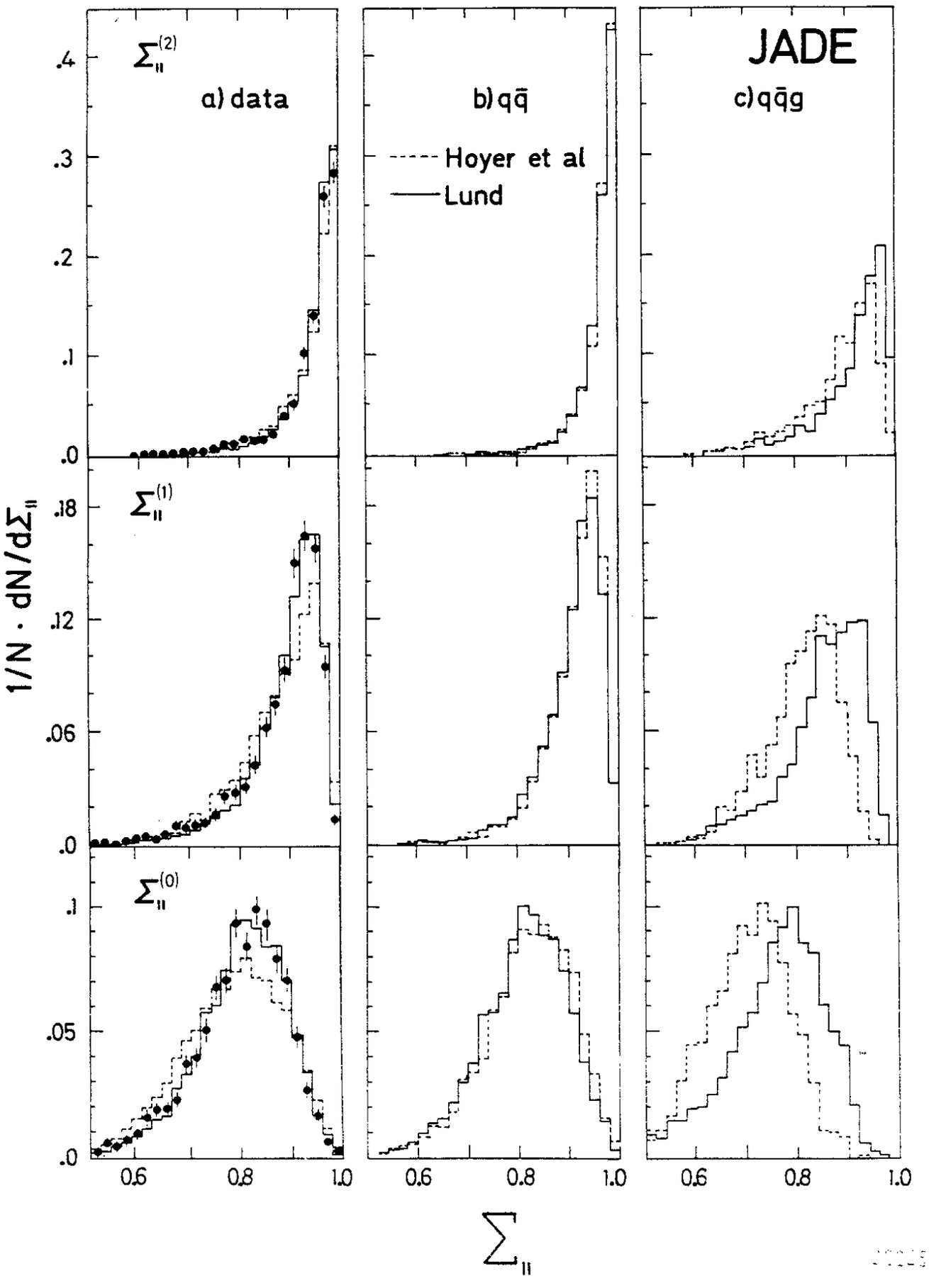
JADE
a) data
b) qq̄
c) qq̄g
Hoyer et al
Lund
$\Sigma_{\parallel}^{(2)}$
$\Sigma_{\parallel}^{(1)}$
$\Sigma_{\parallel}^{(0)}$
$1/N \cdot dN/d\Sigma_{\parallel}$
$\Sigma_{\parallel}$
.4
.3
.2
.1
.0
.18
.12
.06
.05
0.6
0.8
1.0

Fig. 2

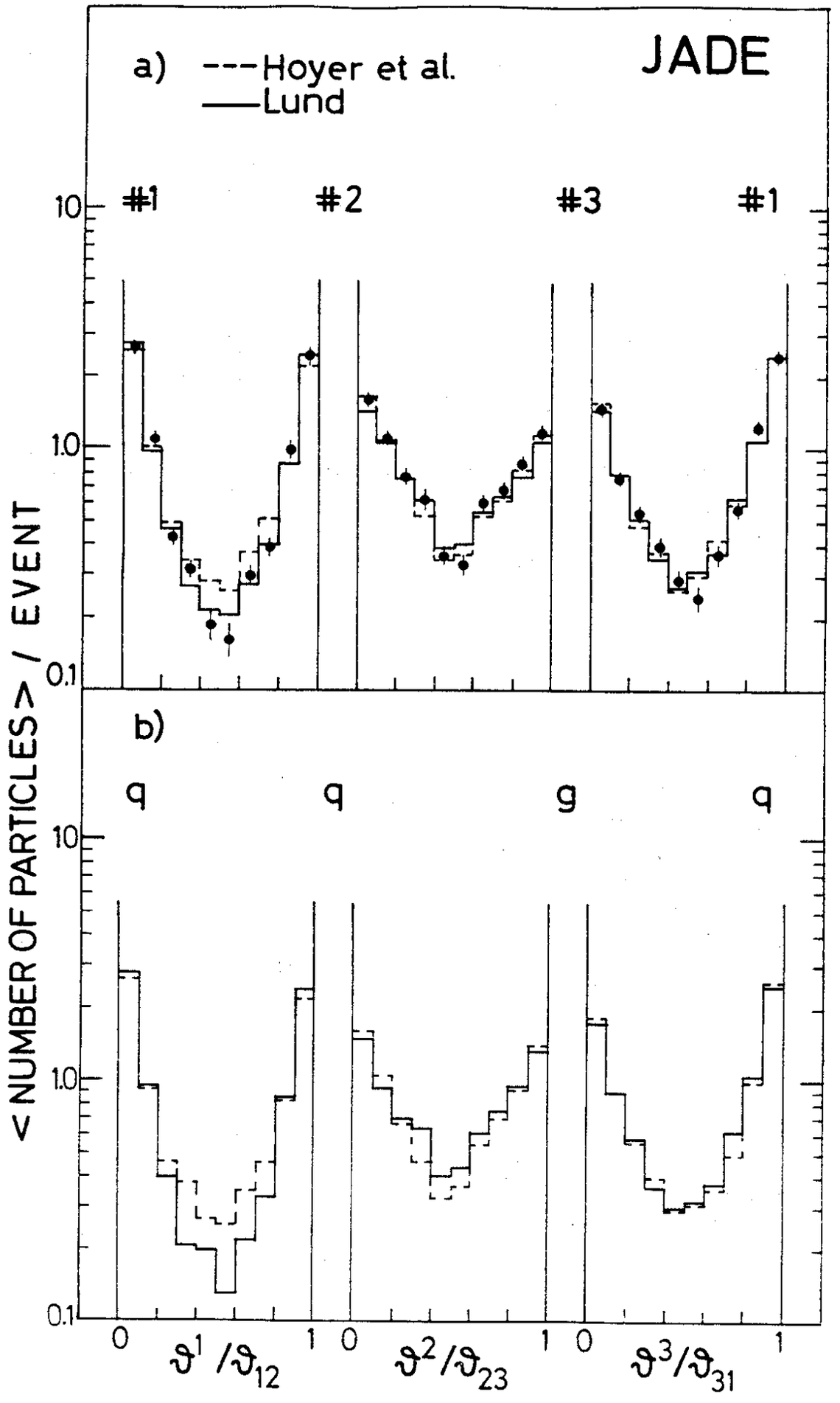
a) ---Hoyer et al.
——Lund
JADE
#1
#2
#3
#1
10
1.0
0.1
b)
q
q
g
q
10
1.0
0.1
< NUMBER OF PARTICLES > / EVENT
0
$\vartheta^1/\vartheta_{12}$
1
0
$\vartheta^2/\vartheta_{23}$
1
0
$\vartheta^3/\vartheta_{31}$
1

Fig. 3